Ultra-low-power ring-based wireless tinymouse

Yifan Li
The University of Tokyo
Tokyo, Japan
yifan217@akg.t.u-tokyo.ac.jp

Masaaki Fukumoto
Microsoft Corporation
Beijing, China
fukumoto@microsoft.com

Mohamed Kari
Princeton University
Princeton, USA
mokari@princeton.edu

Shigemi Ishida
Future University Hakodate
Hokkaidō, Japan
ish@fun.ac.jp

Akihito Noda
Kochi University of Technology
Kochi, Japan
noda.akihito@kochi-tech.ac.jp

Tomoyuki Yokota
The University of Tokyo
Tokyo, Japan
yokota@ntech.t.u-tokyo.ac.jp

Takao Someya
The University of Tokyo
Tokyo, Japan
someya@ee.t.u-tokyo.ac.jp

Yoshihiro Kawahara
The University of Tokyo
Tokyo, Japan
kawahara@akg.t.u-tokyo.ac.jp

Ryo Takahashi*
The University of Tokyo
Tokyo, Japan
takahashi@akg.t.u-tokyo.ac.jp

Figure 1: Overview of picoRing *mouse*, enabling 30-500 uW-class ultra-low-power wireless ring mouse for ubiquitous finger input. The ring can potentially operate over a month on a single charge of a 27 mAh battery (https://youtu.be/7RazVNMx0Ms).

Abstract

Wireless mouse rings offer subtle, reliable pointing interactions for wearable computing platforms. However, the small battery below 27 mAh in the miniature rings restricts the ring's continuous lifespan to just 1-10 hours, because even low-powered wireless communication such as BLE is power-consuming for ring's continuous use. The ring's short lifespan frequently disrupts users' mouse use with the need for frequent charging. This paper presents picoRing *mouse*, enabling a continuous ring-based mouse interaction with ultra-low-powered ring-to-wristband wireless connectivity. picoRing *mouse* employs a coil-based impedance sensing named semi-passive inductive telemetry, allowing a wristband coil to capture a unique frequency response of a nearby ring coil via a sensitive inductive coupling between the coils. The ring coil converts the corresponding user's mouse input into the unique frequency response via an up to 449 uW mouse-driven modulation system. Therefore, the continuous use of picoRing *mouse* can last approximately 600 (8hrs use/day)-1000 (4hrs use/day) hours on a single charge of a 27 mAh battery while supporting subtle thumb-to-index scrolling and pressing interactions in real-world wearable computing situations.

CCS Concepts

• **Human-centered computing** → **Interaction devices**; **Ubiquitous and mobile computing**; **Pointing devices**; • **Hardware** → **Wireless devices**.

Keywords

long-term wearables, ubiquitous finger input, wireless mouse ring, coil-based impedance sensing, semi-passive inductive telemetry

*Correspondence to Ryo Takahashi

UIST '25, September 28-October 1, 2025, Busan, Republic of Korea

ACM ISBN 979-8-4007-2037-6/2025/09
https://doi.org/10.1145/3746059.3747615

ACM Reference Format:
Yifan Li, Masaaki Fukumoto, Mohamed Kari, Shigemi Ishida, Akihito Noda, Tomoyuki Yokota, Takao Someya, Yoshihiro Kawahara, and Ryo Takahashi. 2025. Ultra-low-power ring-based wireless tinymouse. In *The 38th Annual ACM Symposium on User Interface Software and Technology (UIST '25), September 28-October 1, 2025, Busan, Republic of Korea.* ACM, New York, NY, USA, 12 pages. https://doi.org/10.1145/3746059.3747615

1 INTRODUCTION

Mouse devices are basic tools for simple, fast pointing with computers [45]. Integrating tinymouse functionality into wearable form factors such as wristbands, glasses and rings (*e.g.,* Apple Watch, Galaxy Ring) promises always-available essential interactions with wearable computing platforms [20, 50]. Especially, the wireless ring-formed input devices worn on the index finger offer reliable detection of even subtle, privacy-preserved thumb-to-index finger inputs, unlike the wristband and glasses [22, 41]. However, the physical constraint of the tiny ring structure requires the equipment of tens of mAh small batteries, challenging the continuous operation of tens of mW-class power-consuming wireless communication modules. For example, prior wireless rings support below 1-10 hours of continuous wireless communication with Bluetooth Low Energy (BLE), limiting the ring's communication usage to intermittent data transmission [15, 22, 37, 58]. Such an operation is suitable for periodic healthcare monitoring around the rings (*e.g.,* Oura Ring, Galaxy Ring), but not appropriate for the ring-based input interface that requires long-term, real-time communication with other wearables (*e.g.,* smartwatch, HMD).

This paper presents picoRing *mouse*, enabling an ultra-low-power ring-shaped wireless tinymouse with a ring-to-wristband coil-based impedance sensing (see Figure 1). picoRing *mouse* is inspired by a coil-based sensitive impedance sensing named passive inductive telemetry (PIT) [39, 41]. Unlike long-range electromagnetic communication such as BLE and RF backscatter, PIT constructs a short-range but ultra-low-powered inductive link between a pair of a ring coil and a wristband coil. Since the ring coil can send its sensor information to the wristband coil by simply modifying the inductive field generated from the wristband coil, the ring coil does not need active signal transmission with power-hungry communication modules. With the combination of PIT with the ring-based mouse module, picoRing *mouse* enables the ultra-low-powered tinymouse ring with maximum power consumption of approximately 449 µW, enabling continuous operation of approximately 7 (24hrs use/day)-44 (4hrs use/day) days on a single charge of a 27 mAh curved Lipo battery. Furthermore, the shift from a previous full-passive ring design in original picoRing [41] to our semi-passive ring design by integrating an ultra-low-power MCU enables accurate detection of subtle mouse inputs without any physical noise issues (e.g. chattering) and demonstrates picoRing's practical use in real-world scenarios. To facilitate replication and provide comprehensive implementation details, we have open-sourced the current picoRing *mouse*: https://github.com/KawaharaLab/picoRing_mouse.

Our contribution is summarized as follows:

- The design of an ultra-low-powered wireless communication between ring and wristband devices, inspired by sensitive PIT architecture [41].
- The demonstration and technical evaluation of 500 µW-class wireless ring mouse named picoRing *mouse* toward ubiquitous thumb-to-index input.

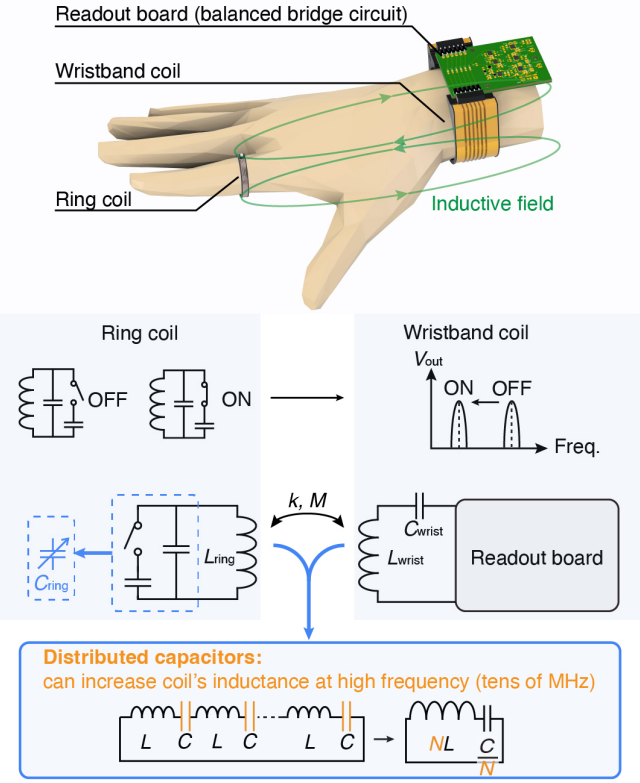

Figure 2: Schematic of passive inductive telemetry (PIT) for ring-to-wristband low-powered wireless connection [41]. PIT allows the wristband coil to stably detect the passive response from the ring –the passive shift in the ring's resonant frequency– through a ring-to-wristband inductive coupling.

2 RELATED WORK

2.1 Wearable Mouse

Wearable mouse has emerged as seamless interaction with wearable computing devices [5, 10, 34]. Specifically, the smart accessories such as rings or wristbands allows users to control and interact with technology through subtle finger and hand movements [14]. Wristbands have been explored for detecting finger movements using various technologies, including force measurement [7], electromagnetic waves [21], inertial sensing [23], capacitive coupling [55], and electromyography (EMG) [35]. While these methods can detect gestures, they face challenges in accurately capturing subtle finger motions due to the distance from the fingers. Machine learning and sensor fusion techniques have been employed to improve gesture recognition accuracy, though they often require dynamic motions and frequent calibration [50]. In contrast, rings provide a closer proximity to the fingers, allowing for more precise detection of subtle movements even with simple sensors and algorithms [20, 41]. This close-range sensing enables stable interaction without causing user fatigue, making them suitable for everyday use.

Table 1: Technical comparison of wireless ring-based input devices. To the best of our knowledge, picoRing *mouse* is the first long-term wireless tinymouse ring achieving an ultra-low-powered operation below 1 mW.

Ring	Components	Wireless connection	Ring's maximum power (mW)	Available input interface	User and session independence
Galaxy Ring	Ring	BLE	-	Finger tap	✓
ElectroRing [20]	Ring	BLE	220	Finger press	✓
Ring-a-Pose [51]	Ring	BLE	148	Finger pose	✓
OmniRing [58]	1-5 rings	BLE	40/ring	Finger pose	✓
IRIS [22]	Ring	BLE	26	Vision	✓
MouseRing [22]	Ring	BLE	−10	Finger slide	✓
FingeRing [9]	5 rings & wristband	Intrabody communication	**1.8/ring**	Finger tap	△ Unstable link under RF noises
Nenya [1]	Ring & wristband	Static magnetic field	**0**	Finger scroll	× Unstable link under magnetic noises
AuraRing [33]	Ring & wristband	Near-field inductive coupling	**2.3**	Finger pose	✓
TelemetRing [39]	5 rings & wristband	PIT	**0/ring**	Finger tap	✓
picoRing [41]	Ring & wristband	PIT	**0**	Finger press **or** scroll	✓
picoRing *mouse*	Ring & wristband	semi-PIT	**0.45**	Finger press **and** scroll	✓

2.2 Wireless Ring

Ring-formed mouse devices have long been investigated within the HCI community. The exploration of the previous mouse ring can be divided into two categories: i) ring-based sensing techniques such as computer vision [3, 19, 38], inertial sensors [28, 37], ultrasound [51, 53], and electromagnetic wave [4, 46] and ii) low-powered wireless ring design using RF backscatter [2, 8, 30], near-field communication (NFC) [24, 29, 52], intrabody communication [10, 44], and magnet-based tracking [1]. The ring-based finger sensing demonstrates high-fidelity microgesture recognition compared to the wristband- and glasses-based finger sensing [20]. However, the long-term operation of the low-powered wireless rings is still challenging [47]. Specifically, μW-class RF backscatter and magnet-mounted ring need a large antenna and a bulky magnet, which is hard to fit in the small ring [1, 32]. Moreover, the magnet-based tracking via exposed static magnetic field is easily influenced by the surrounding magnetic noises such as electrical appliances, impairing the tracking accuracy of the magnet position or orientation [48]. mW-class NFC supports small tag design, but the communication range is a few centimeter-scale [13, 40, 54]; such a short-range link cannot construct ring-to-wristband communication. Intrabody communication [10, 44], which uses capacitive body as a signal path, can transmit signal with μW-class ultra-low-power throughout the body [25], but both the RF presence of other electronic devices and the daily items such as wooden desk and wall can impair the capacitive signal path, causing signal degradation, reduced transmission range, or even data loss [20].

2.3 Passive Inductive Telemetry

picoRing [41], which is most similar to this paper, extends the coil-based communication distance by using PIT [26, 39, 42]. PIT consists of a pair of a fully-passive ring coil and a wristband coil, allowing the wristband to detect the passive response of the ring coil (see Figure 2). Specifically, ring coil, which consists of a resonant *LC* tank connected to a physical switch, converts the thumb-to-switch inputs into the change of the ring's resonant frequency, defined as $f = 1/(2\pi\sqrt{LC})$, without any active electrical components; ON/OFF of the switch connected to the chip capacitor allows the passive change of the total capacitance of the ring coil. Because the ring's resonant change causes the impedance change in the wristband coil through ring-to-wristband inductive coupling, the wristband coil can recognize the thumb-to-switch input by detecting the frequency peak in its impedance characteristics, appeared around the ring's resonant frequency. Because the ring away from the wristband inevitably couples with the wristband through a significantly weak inductive coupling, prior picoRing [41] has proposed the sensitive PIT by combining a sensitive coil with distributed capacitors [6] with a sensitive impedance measurement circuit named balanced bridge circuit [39]. The sensitive coil, which has a large turn number or large inductance at a high resonant frequency (*i.e.,* tens of MHz) by inserting multiple chip capacitors into a single long coil, can increase the passive response from the ring coil. Furthermore, the bridge circuit, which uses a differential circuit structure and impedance balancing technique, can be sensitive to the small impedance change of the wristband coil. With these configuration, picoRing constructs stable ring-to-wristband wireless

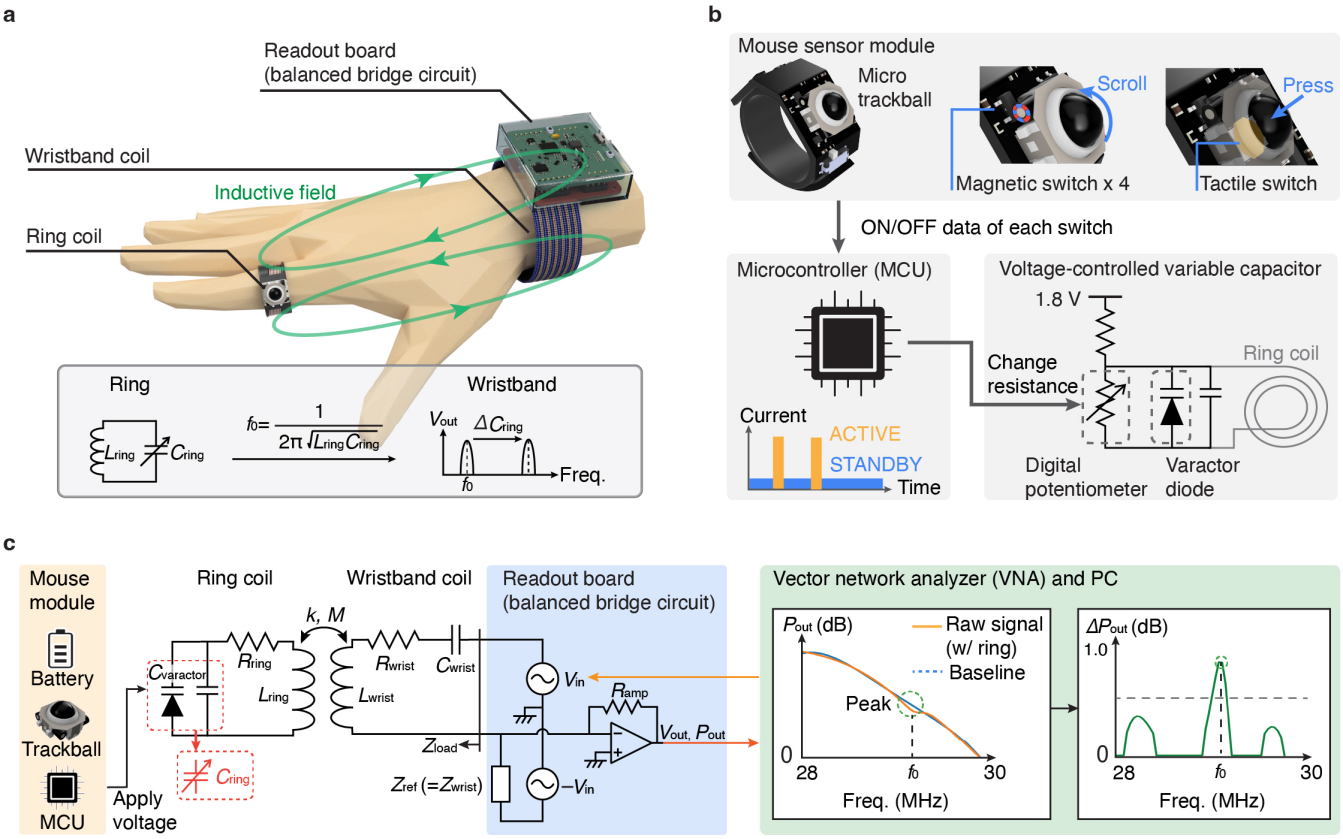

Figure 3: Design overview of picoRing *mouse*. (a) Schematic of picoRing *mouse*, consisting of a pair of a ring coil and a wristband coil connected to a readout board (impedance measurement circuit). (b) Illustration of working principle of the ring coil to convert the mouse input into unique shift of the ring's resonant frequency. (c) Circuit diagram of picoRing *mouse*.

link despite proximity to metallic items and electrical appliances. For more detail, please refer to [41].

While picoRing employs the passive mechanical switch as the battery-free variable capacitor, the ring without any digital computational components, e.g., microcontroller (MCU) and analog-to-digital converter, is challenging to support mouse-like multi-modal inputs. This is because the ring-sized input sensors available in the commence needs the battery-assisted electrical sensors; the miniaturization of multi-modal mechanical switch is hard due to the spatial challenges. Therefore, prior picoRing [41] requires the users to change the different types of rings (*e.g.*, picoRing *press*, *slide*, *joystick*, and *scroll*) according to the target finger inputs. By contrast, picoRing *mouse* can support multi-modal thumb-to-index inputs with a single ring by integrating low-powered, miniaturized mouse sensor and signal encoding circuit into the prior picoRing system. Table 1 shows the technical comparison among ring-formed mouse devices. **To the best of our knowledge, picoRing *mouse* is the first to demonstrate the ultra-low-powered wireless mouse ring below 500 uW for long-term ubiquitous finger input interface.**

3 SYSTEM DESIGN

picoRing *mouse* consists of two main components (see Figure 3a): 1) a ring coil with a mouse module, which changes its frequency response based on the thumb-to-index inputs, and 2) a wristband coil that detects the unique peak in the frequency response generated by the ring's resonance. The working principle of picoRing *mouse* is as follows: First, the wristband coil generates a weak inductive field to couple with the nearby ring coil. When the user scrolls or presses the mouse module mounted on the ring, the MCU connected to the mouse module detects either the scrolling or pressing via the magnet or tactile switch, transforming the mouse input into a unique frequency response (*i.e.*, the change in the ring's resonant frequency) via a voltage-controlled variable capacitor (see Figure 3b). Owing to the inductive coupling, the wristband coil connected to a sensitive impedance measurement module obtains the frequency response. Since the ring's frequency response appears as a sharp frequency peak at the ring's resonant frequency in the frequency characteristics of the wristband's impedance, the wristband coil enables to recognize the mouse input (*i.e.*, pressing and 2D scrolling) as a unique peak output.

3.1 Ring-to-wristband Wireless Communication

picoRing *mouse* extends the PIT system in a semi-passive manner. While the prior PIT features the full-passive design of the ring coil by modifying the ring-to-wristband inductive field with a full-passive modulation circuit composed of tactile switches. In contrast, picoRing *mouse* employs the semi-passive modulation approach, which modifies the inductive field with a low-powered digital modulation circuit composed of a battery-assisted voltage-controlled variable capacitor. Note that the semi-passive modulation approach does not use the active signal transmission circuit. Unlike full-passive modulation, the semi-passive modulation can transmits the sensor information as digital signals. Specifically, picoRing *mouse* uses a simple frequency-shift keying, which encodes the multi-modal mouse input into a corresponding frequency shift based on the voltage-controlled variable capacitor.

Let us explain how the ring coil can influence the wristband coil in the frequency-shifting manner. When the ring coil resonates at f_0 inductively couples with the wristband coil, the input impedance of the wristband coil, Z_{load}, can be expressed as follows:

$$Z_{\text{load}}(\omega) = Z_{\text{wrist}}(\omega) + \Delta Z_{\text{wrist}}(\omega) \tag{1}$$

$$\Delta Z_{\text{wrist}}(\omega) = \frac{(\omega M)^2}{Z_{\text{ring}}(\omega)} \tag{2}$$

$$Z_{\text{wrist}}(\omega) = R_{\text{wrist}} + j\left(\omega L_{\text{wrist}} - \frac{1}{\omega C_{\text{wrist}}}\right) \tag{3}$$

$$Z_{\text{ring}}(\omega) = R_{\text{ring}} + j\left(\omega L_{\text{ring}} - \frac{1}{\omega C_{\text{ring}}}\right) \tag{4}$$

where Z_{wrist} and Z_{ring} are the total impedance of the wristband and ring coils, respectively, ω $(= 2\pi f)$ is the angular frequency, M is the mutual inductance between the ring and wristband coils. Z_{ring} can be simplified as R_{ring} at f_0 because $\omega_0 L_{\text{ring}} - 1/(\omega_0 C_{\text{ring}})$ is 0 in the resonance state. As a result, Equation 2 can be also simplified at $\omega_0 = 2\pi f_0$ as follows:

$$\Delta Z_{\text{wrist}}(\omega_0) = \frac{(\omega_0 M)^2}{R_{\text{ring}}} \tag{5}$$

Equation 5 indicates ΔZ_{wrist} increases significantly around ω_0, resulting in the sharp peak in the frequency characteristics of ΔZ_{wrist} around ω_0. However, similar to picoRing [41], the extremely weak inductive coupling makes ΔZ_{wrist} too small to detect through a standard impedance measurement circuit.

To detect ΔZ_{wrist}, or small variations in Z_{load}, the balanced bridge circuit is useful [39, 41]. The balanced bridge circuit, shown in Figure 3c, can be sensitive to only the small impedance change, by an impedance balancing process between the wristband coil and embedded chip components on the bridge circuit ($Z_{\text{wrist}} = Z_{\text{ref}}$). With this impedance balance, the output of the bridge circuit, V_{out} and P_{out}, at ω_0 can be expressed with $Z_{\text{wrist}} \gg \Delta Z_{\text{wrist}}$, Equation 1, and Equation 2:

$$V_{\text{out}}(\omega) = -R_{\text{amp}}\left(\frac{V_{\text{in}}}{Z_{\text{load}}} - \frac{V_{\text{in}}}{Z_{\text{ref}}}\right) \tag{6}$$

$$\approx R_{\text{amp}} \frac{\Delta Z_{\text{wrist}}(\omega)}{Z_{\text{ref}}^2} V_{\text{in}} \tag{7}$$

$$\downarrow \text{convert } V_{\text{out}} \text{ to } P_{\text{out}} \text{ (dB)}$$

$$\Delta P_{\text{out}}(\omega)(\text{dB}) \approx \begin{cases} 0 \ (\omega \neq \omega_0 \text{ or w/o ring coil}) \\ \Delta Z_{\text{wrist}}(\omega_0) \ (\text{dB}) \ (\omega \approx \omega_0) \end{cases} \tag{8}$$

where V_{in} is the input voltage of the bridge circuit, R_{amp} is the amplifier factor. Note that $Z_{\text{ring}}(\omega) \gg (\omega M)^2$ is valid under condition $\omega \neq \omega_0$ because Z_{ring} has the large imaginary part at non-resonant frequency and M is so small in the situation where the ring coil is away from the wristband coil. Equation 8 indicates that the wristband coil can reliably detect the ring's resonant frequency through output (P_{out}(dB)) of the bridge circuit. Therefore, the ring coil, which changes its resonant frequency with the variable capacitor, can send its mouse sensor information to the wristband coil in the frequency-keying way. Moreover, the semi-passive signal transmission of the ring coil, which modifies the inductive field from the wristband coil in the load-modulation way, can save power for signal transmission unlike the active signal transmission.

3.2 Ring

The ring coil consists of an 8-turned resonant coil with distributed capacitors and the mouse module equipped with a small trackball (EVQWJN007, Panasonic) supporting up, down, right, left scrolling and pressing interactions. When users scroll or press the trackball in the mouse module, the trackball either i) converts the scroll rotation of the trackball into rotation of cylindrical magnets with alternating polarity distribution or ii) turns on the tactile switch reacting to the user press of the trackball (see Figure 3b). The magnetic switch (CT8132BL, Allegro MicroSystems) below each magnet sends the magnet rotation data to an ultra-low-power MCU (STM32L011F4U6, STM) along with the ON/OFF data of the tactile switch, and then, according to the input type, the MCU applies a different corresponding voltage to a varactor diode (SMV1253, Skyworks) by a digital-potentiometer-based voltage divider circuit (AD5160, Analog Devices). The varactor diode, which varies its capacitance from 27 pF to 69 pF based on the applied voltage, can change the C_{ring} by being connected in parallel to one of the distributed capacitors in the ring coil.

The ring coil provides five physical inputs: none, scroll down, up, left, right, and press. The resonant frequency for each input is set to 27.32 MHz, 27.46 MHz, 27.60 MHz, 27.83 MHz, 28.23 MHz, and 28.47 MHz, respectively, within the impedance-balanced frequency band. The inductance (L_{ring}) and resistance (R_{ring}) of the ring coil at 28.2 MHz are 2.6 µH and 3.5 Ω, respectively. Note that the ring coil is tilted with approximately 20°, mitigating the misalignment between the ring and wristband coils when the hand is grasped for thumb-to-index input. Scrolling diagonally results in the simultaneous scrolling of adjacent horizontal and vertical magnets. For instance, when scrolling diagonally to the upper right, both the

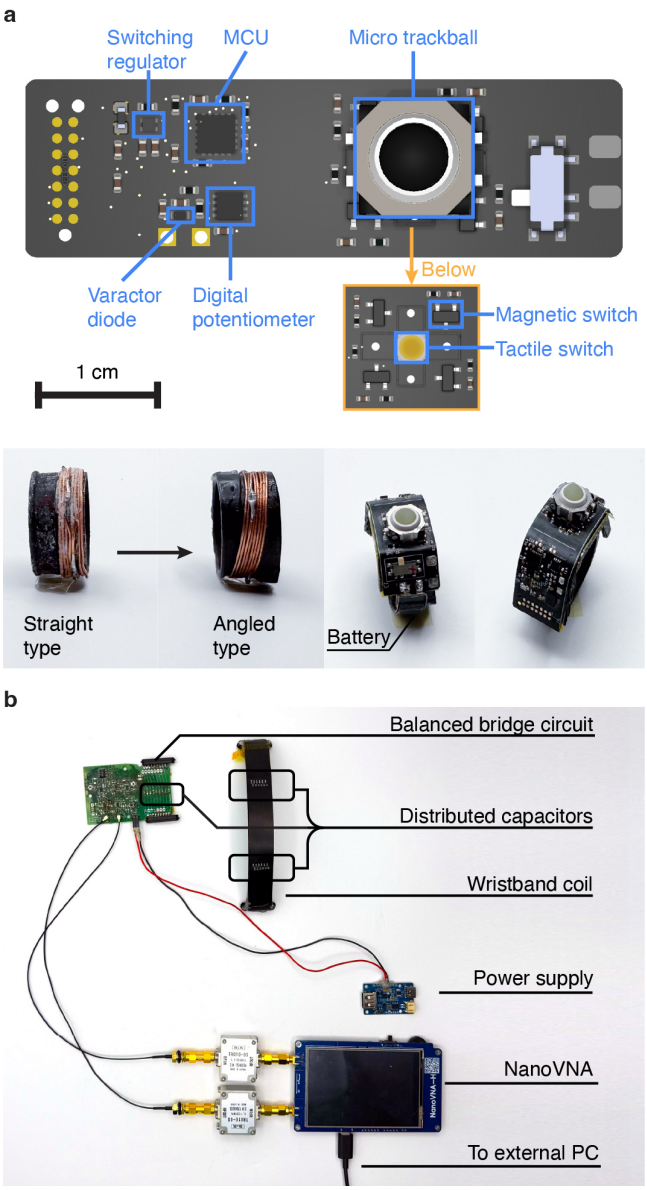

Figure 4: Prototype photograph of our (a) ring coil with a 45 × 14 mm flexible PCBs including a micro trackball, mouse sensor module, MCU, varactor diode, digital potentiometer, and switching regulator, and (b) wristband coil implemented flexible PCBs. The flexible PCBs are mounted to the 3D-printed wristband, and the wristband coil is connected to the readout board, composed of the balanced bridge circuit, NanoVNA, and external PC.

up and right magnets move concurrently. The MCU decodes this diagonal scrolling into vertical and horizontal scrolling in turn.

The ring coil has two types of operation modes: ACTIVE mode and STANDBY mode. In the ACTIVE mode, the ring coil continuously streams data to the wristband coil with 200 fps. By contrast, in the STANDBY mode, the timer in the MCU periodically awakens to check the receiving data from the connected magnet switch. picoRing basically waits in the STANDBY mode and transits to ACTIVE mode when the user inputs to the mouse module. When there is no signal change in the magnet switch for 30 s, picoRing backs to the STANDBY mode. Note that the MCU clock in the ACTIVE and STANDBY modes is set to 524 kHz and 32 kHz, respectively.

Table 2: Power consumption of the ring coil hardware.

Component	STANDBY (μW)	ACTIVE (μW)
MCU (STM32L011F4U6)	1.8	252
Mouse sensor module (4 × CT8132)	7.9	7.9
Digital voltage divider (MAX5394)	1.8	36
Power management (TPS62843)	0.63	0.63
Estimated total	> 12	> 296
Measured total@4.2 V	**25**	**449**

3.3 Wristband

The wristband coil consists of a 6-turned flexible resonant coil mounted on a 3D-printed flexible wristband and the readout board connected to a mobile vector network analyzer (VNA) (NanoVNA-H4). To recognize the ring's mouse state, the wristband coil detects the ring's frequency peak (f_0) by monitoring the frequency sweep signal ranging from 27.0 MHz to 28.5 MHz with an input power of 0.2 mW, the frequency bandwidth of 4 kHz, the sampling number of 101, and the sampling rate of 20 fps. This setup for fast VNA readout enables the reliable detection of subtle and fast finger scrolling but, the frequency peak sometimes shifts because the large frequency step resolution of the NanoVNA without noise reduction sometimes fluctuates the frequency peak data. To address this, we've designed the ring's six resonant frequencies with a enough frequency space of 0.2 − 0.4 MHz, as described in § 3.2.

The wristband created by FDM 3D-printing of TPU filament is designed in the ellipse shape with 6.2 cm width, 5.2 cm height, and 1.9 cm length to fit in the middle-sized adult hands. The wristband coil is connected to the readout board via two 6 pin magnetic connectors (DIY Magnetic Connector, Adfruit). The reader board consists of the bridge circuit composed of six amplifiers (LTC6228, Analog Devices), magnetic connectors, and an external PC (Macbook Air). The NanoVNA sends the power spectrum of the frequency response to the connected external PC, which analyzes the frequency peak in the power spectrum, similar to the same peak detection algorithm as picoRing [41]. In total, the resonant frequency, inductance (L_{wrist}) and resistance (R_{wrist}) of the wristband coil connected with eighteen 150 pF distributed capacitors and a 47 Ω resistor in series are 27 MHz, 4.2 μH, and 49 Ω, respectively, and the measured power consumption of the bridge circuit and NanoVNA are 0.33 W (= 3.3 V × 0.1 A) and 1.0 W (= 5 V × 0.2 A), respectively. The current wristband coil created by the flexible PCBs and TPU-based band would have the challenge of wearability and stretchability. The use of stretchable textile coil [16, 42] is promising for high biocompatibility for the skin.

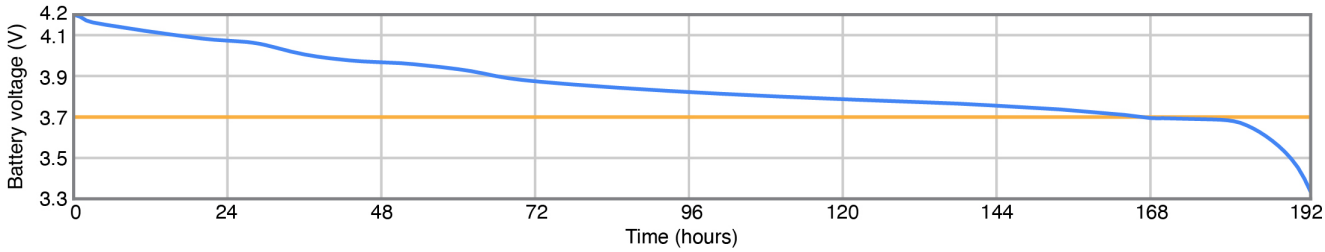

Figure 5: Data plot of battery voltage over the operation time of our wireless ring.

Table 3: Estimation of battery lifespan of the ring coil driven by 20 mAh or 27 mAh batteries, respectively.

Operation time of ACTIVE mode (hrs/day)	Battery lifespan w/ 20 mAh (hrs)	Battery lifespan w/ 27 mAh (hrs)
24	167[1]	225
8	451	609
4	784	1058

[1]: We measured the actual battery lifespan for this case.

4 TECHNICAL EVALUATION

4.1 Operation Time of picoRing *mouse*

First, we measured how long picoRing *mouse* can operate. To calculate the expected battery life during usage, we first connected the battery terminals of picoRing *mouse* to a digital multimeter (34410A, Keysight). The measured power consumption at 4.2 V during ACTIVE and STANDBY mode is measured to be approximately 449 µW (=4.2 V×107 µA) and 35 µW (=4.2 V×8.4 µA), respectively. Then, we estimated the battery lifespan hours for three types of different ACTIVE operation time of picoRing *mouse*. For reference, we measured the battery lifespan hours when picoRing *mouse* operates continuously in ACTIVE mode. The battery lifespan is calculated from when the LiPo battery is fully charged at 4.2 V until it drops below 3.7 V (see Figure 5). To maintain the ACTIVE mode, the MCU is instructed to keep the digital voltage divider ON, i.e., shifting up the resonant frequency of the ring-shaped coil from 27 MHz (*i.e.*, the digital voltage divider is OFF) to 29 MHz. Note that the magnetic scroll detector is also kept running continuously. The measured time is approximately 167 hours, i.e., 7 days with the fully-charged 20 mAh Lipo battery (UFX150732).

Based on the result of power consumption and battery lifespan in continuous ACTIVE mode, Table 3 shows the expected battery lifespan for the different operation hours (*i.e.,* 4, 8, or 24 hours per day). The lifespan hour is estimated based on two types of battery capacity: 20 mAh and 27 mAh, both of which is widely used in commercially-available smart ring products. Based on the practical usage time of a mouse without causing tendinitis, which is approximately 4-8 hours per day [11, 31, 49], picoRing *mouse* has the potential to operate for approximately 451 (8 hrs/day)-1058 (4 hrs/day) hours, or over a few weeks or one month, on a single charge of 20 – 27 mAh battery.

4.2 SNR of picoRing *mouse*

We then evaluate the signal-to-noise ratio (SNR) of picoRing *mouse* for user's scrolling and pressing interactions, input power, distance between the ring and wristband, the finger bending, and public environments. Similar to [41], the SNR was calculated as follows using S21 100 outputs (P_{out} (dB) = $20\log_{10} V_{\text{out}}$) of the VNA:

$$\text{SNR(a.u.)} = \frac{\text{mean}\left(P_{\text{out w/ ring}}\right) - \text{mean}\left(P_{\text{out w/o ring}}\right)}{\text{std}\left(P_{\text{out w/o ring}}\right)}$$

Here, we consider that the SNR over 10 can support high-fidelity recognition over 99% accuracy, referring to [41]. Also, we decouple the readout board with the common ground using the RF transformers (T1-1-X65+, Mini Circuits). Figure 6a shows the time-series SNR and the average SNR for the pressing and 2D scrolling inputs. The average SNR was calculated using data collected over a 5-minute period from three invited participants with almost similar hand sizes (one woman and two men, 20s). The result shows that the average SNR for each input is over 10 dB with minimal variations, indicating that picoRing *mouse* can support high-fidelity recognition of thumb-to-mouse finger inputs for a similar hand size. To be available for various hand sizes, we will quantitatively explore how the coil size can affect the SNR using those like electromagnetic simulators.

Next, we measured how the distance and orientation of the ring coil influence the SNR of picoRing *mouse*. Original picoRing [41] have shown that the SNR characteristics is almost the same with or without the hands, thanks to the inductive inherent robustness to dielectric human presence. Therefore, we conducted this evaluation without human hands to easily adjust the distance and orientation between the coils. Specifically, we prepared a set of jigs to change the distance and orientation of the ring coil by the 3D printer (see Figure 6b). The range of he distance is from 10 cm to 20 cm in step of 1 cm in addition to varying the angle of the ring coil from −30° to 60° in step of 30°. We prepared the two types of ring coils: straight-type coil and tilted-type coil with the coil angled about 20° to the vertical axis of the ring. Because the thumb-to-index input, which is typically performed with the finger in the bent position, can cause misalignment between the ring and wristband coils, weakening magnetic coupling, the tilted ring with the coil angled to the vertical axis enables to maintain the alignment and strengthen the inductive coupling. Note that the ring's resonant frequency is tuned at 28 MHz. The result shows that the available distance is estimated to be approximately 14 cm because the SNR is over 10 against up to

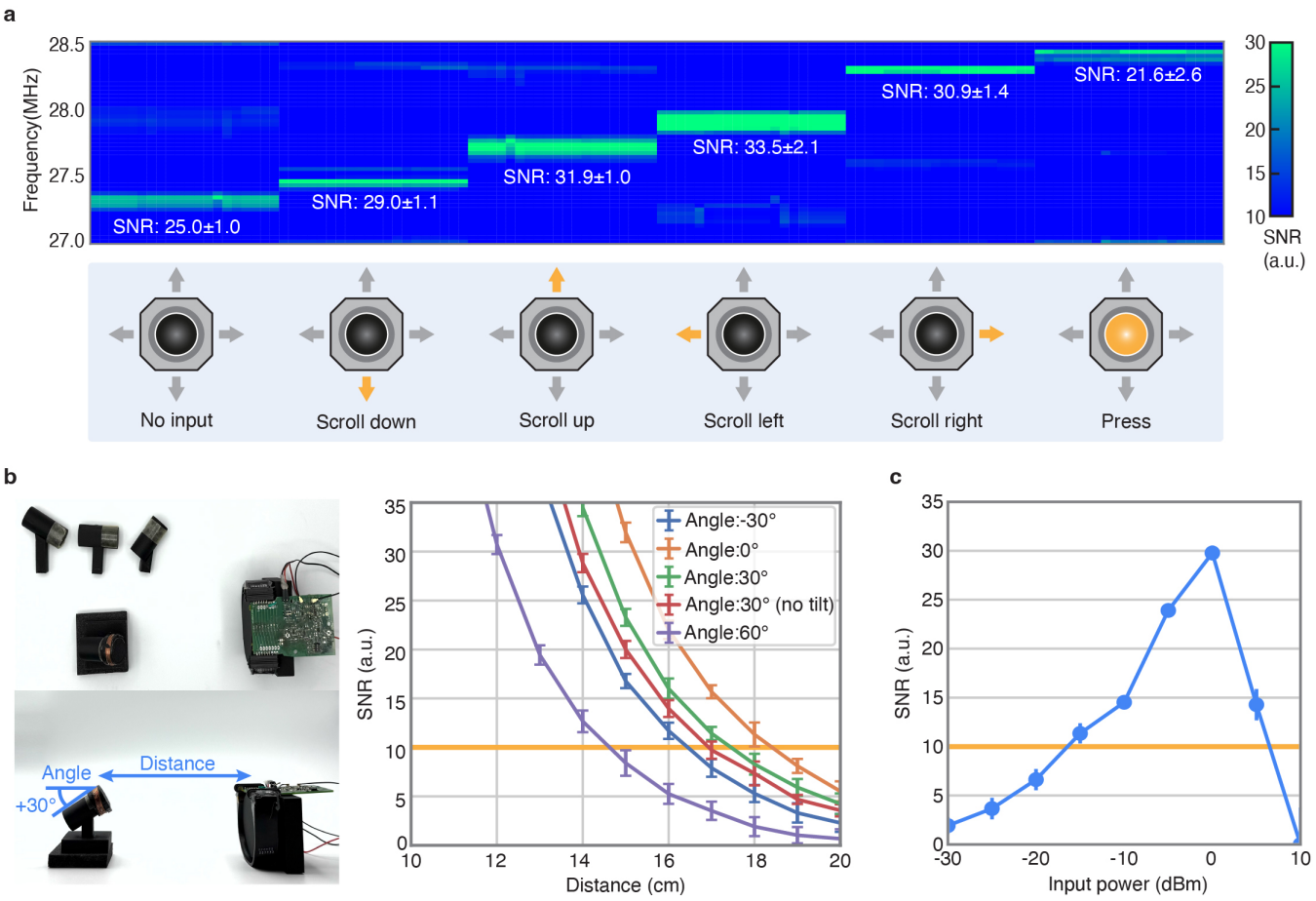

Figure 6: Signal-to-noise ratio (SNR) of picoRing *mouse* in controlled environments. (a) Time-series and average SNR for scrolling and pressing interactions for three users. (b) SNR for the distance and angle between the ring and the wristband coils. (c) SNR for the input power of the wristband coil.

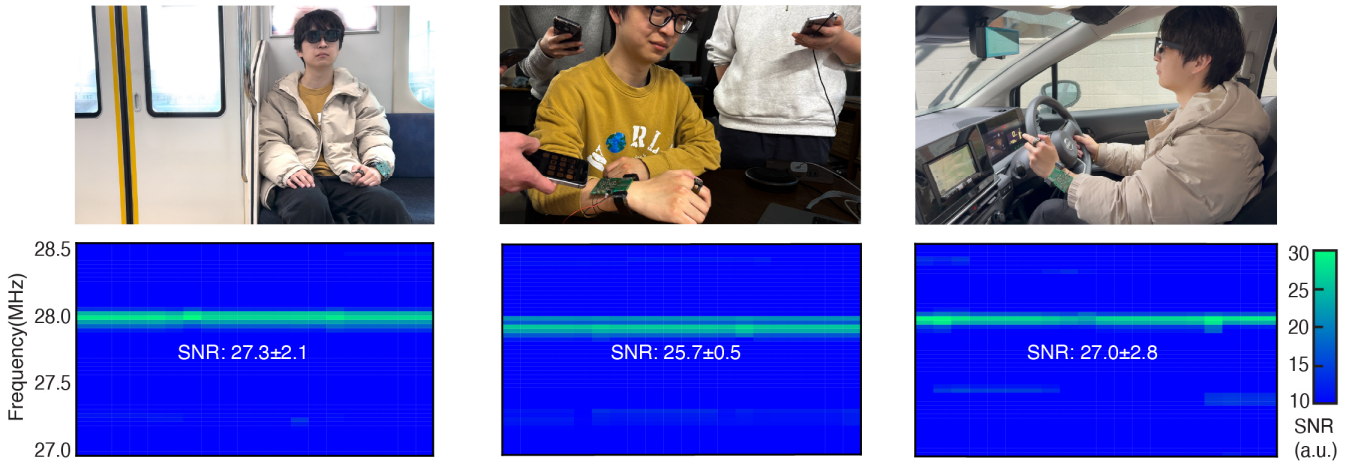

Figure 7: Signal-to-noise ratio (SNR) of picoRing *mouse* against the three types of electromagnetically-noisy sessions in real-world wearable computing.

Figure 8: Application examples of picoRing *mouse*.

60° finger bending. These available distance and angle provided by picoRing *mouse* are well-suited for the reliable thumb-to-index input during the typical middle-sized hand movements. Furthermore, the tilted ring could increase the SNR by approximately 3 when the finger is bent by around 30° because the measured inductive coupling coefficient (k) increases from 0.0031 to 0.0039.

Then, we evaluated the SNR varying the input power of the wristband coil from −30 dBm (= 1 µW) to 10 dBm (= 10 mW) in steps of 5 dB (see Figure 6c). The distance and angle between the ring and the wristband is set to 14 cm and 30°, respectively. The result indicates the input power ranging from −15 dBm (=30 µW) to 5 dBm (=3.2 mW) achieves the SNR over 10, although the high input power over 10 dBm (= 10 mW) unfortunately causes the decrease of SNR due to the fluctuation of the amplifier in the bridge circuit. To save the operational power of the bridge circuit, we chose −7 dBm (= 0.2 mW) as the input power of the NanoVNA, from the available power options in the NanoVNA.

Finally, we measured the SNR during the daily usage. Although the SNRs for proximity to metallic items and electrical appliances are shown to be robust in picoRing [41], our focus is on measuring the SNR against electromagnetically-noisy situations in real-world wearable computing scenarios. Here, we consider the following three situations: using the ring while 1) seated in a train, 2) standing in crowded areas in addition to being surrounded by the multiple smartphones, and 3) driving a car. Note that the measured noise level in these situations is approximately 20 dBm/Hz higher than in typical environments. Figure 7 shows the time-series SNR spectrum and average SNR for these situations, based on data from a single user (20s, man). The result indicates that picoRing *mouse* successfully detects a sharp peak at 28 MHz with the sufficient SNR over 25 despite proximity to the metallic items (*e.g.,* steering wheels) and electrical appliances (*e.g.,* laptops, smartphones, electronic control units in the cars and trains).

5 APPLICATION EXAMPLES

picoRing *mouse* offers a significant advantage in providing long-term continuous operation on a single charge, while reliably detecting subtle thumb-to-index inputs. Therefore, its primary application is ubiquitous finger-based interaction systems, particularly when integrated with augmented reality (AR) glasses or head-mounted displays (HMD) (see Figure 8). AR glasses and HMDs often rely on dynamic hand gestures for scrolling interactions, which can lead to fatigue over time. In contrast, picoRing *mouse* offers subtle finger inputs that enable comfortable, long-term interactions while preserving user privacy. This makes it an ideal solution for seamless engagement with digital content. Additionally, the device's efficient power management allows frequent and natural use without concerns about battery life, enhancing its practicality in everyday AR and HMD applications. Figure 8 shows some application examples of picoRing *mouse*. The discreet nature of ring inputs are not easily noticed by the surroundings, minimizing any disruption to those nearby. For example, in an airplane or train, a user discreetly interacts with a personal screen using the picoRing *mouse*, allowing for private control without disturbing nearby passengers. Even in an urban crowded space, users navigate a large public display or AR map with the picoRing *mouse*, seamlessly interacting with digital content (https://youtu.be/7RazVNMx0Ms).

6 DISCUSSION

Dual-device requirement. picoRing *mouse* requires users to attach the two types of wearable devices—ring and wristband—unlike the standard wearables like smartwatches and smart rings. Given that many users already wear wristbands throughout the day for health and fitness tracking, as well as for convenient visual displays, the burden of wearing an additional ultra-low-power ring that requires minimal charging is quite light, making it easy to incorporate wearing a pair of the ring and the wristband into daily routines.

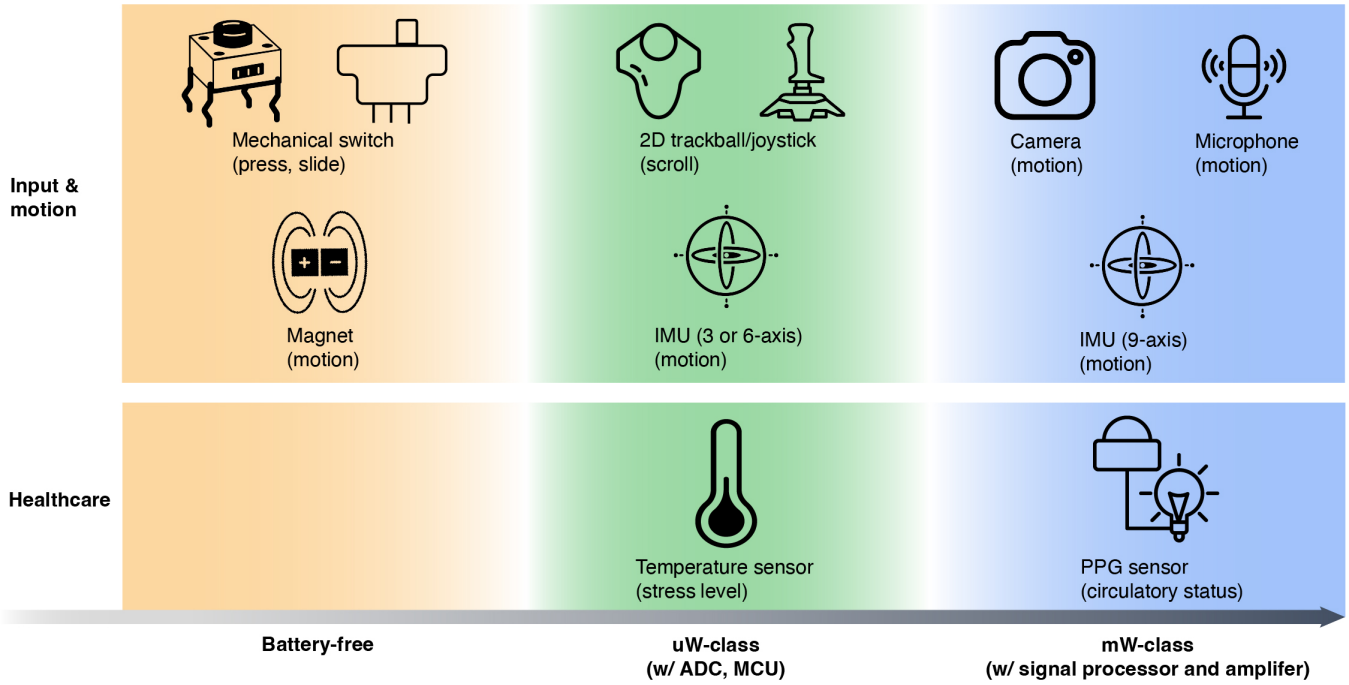

Figure 9: Examples of ring-sized small sensors for input & motion or healthcare purpose.

Bulky and power-consuming readout board. Currently, our readout board, which includes the bridge, VNA, and the external PC, requires a smartphone-sized NanoVNA. However, the board could be miniaturized to fit into a smartwatch. NFC, which hardware is optimized for the coil-based communication [40], could decrease the total power consumption less than 50 mW [18, 57]. Such a low power operation of the wristband coil could allow the integration of our wristband system into the commercially-available smartwatch, which is typically driven by about 500 mAh-class Lipo battery [12].

Wireless charging while in use. Wearable devices often recharge naturally when not in use, such as earbuds placed in dedicated charging cases. However, rings and wristbands are typically worn continuously, making this more challenging. The integration of a wearable power transmission system such as charging-enabled textiles could achieve the continuous power supply to picoRing *mouse* in the use [27, 36, 43]. This would ensure that picoRing *mouse* remains powered throughout daily activities, enabling to be worn continuously as a fashion accessory.

Limited user study. In the current study, we primarily focused on measuring the SNR related to mouse input. Unlike antenna-based wearable devices operating at higher frequencies (e.g., 2.4 GHz or 920 MHz) which are significantly affected by the human body's high dielectric loss, our coil-based system experiences almost no electromagnetic interference from a person. This means the signal-to-noise ratio (SNR) and frequency response remain largely unchanged whether the device is worn or not by human hand. One potential user study will be a multi-factorial repeated-measures ANOVA to assess additional aspects such as ease of use, social acceptance, and fatigue [4]. These evaluations will provide further understanding of the picoRing *mouse* in various real-world scenarios, helping to refine its design and improve user experience.

Extension of ring functionality. picoRing *mouse* has the potential to become a versatile ultra-low-powered wearable platform for a wide range of applications by integrating various low-powered sensors. For instance, by incorporating IMUs [37, 56] or speaker [51], picoRing can be transformed into motion sensing rings (see Figure 9). Additionally, integrating PPG or temperature sensors could transform it into a healthcare ring. Furthermore, wearing picoRing *mouse* on both hands can enable wearable VR/AR interface even in public spaces, by converting the user's subtle mouse input to extended 3D hand dynamic posture [17].

Optimization for further ring's low-powered operation. We are utilizing the ultra-low-powered MCU (STM32L011F4U6, STM), and there is still room for reducing power consumption in both hardware and software aspects. For instance, we can lower the operating voltage from 1.8 V to 1.2 V or reduce the MCU's clock speed. We would explore these options to increase further battery runtime, resulting in a decrease of the battery size.

Error handling in frequency-shift keying. The current frequency-shift keying in our ring-to-wristband communication is so simple, using different frequencies to send the digital information from the mouse sensor. This simplicity presents several challenges, such as security concerns and data integrity issues. Furthermore, the slow data rate of 10 – 200 bps in the current picoRing *mouse* allows the high SNR against electromagnetic noise from nearby devices. However, the fast communication at 10 – 200 kbps-level such as for IMU data would make picoRing *mouse* vulnerable to electromagnetic noise, causing a significant drop in SNR. To ensure reliable and fast

ring-to-wristband communication, error handling techniques such as forward error correction would be commonly available.

7 CONCLUSION

This paper presents picoRing *mouse*, an ultra-low-power ring-based finger input device. By combining semi-PIT-based ring-to-wristband low-powered wireless communication with the low-powered mouse module, picoRing *mouse* achieves long-term operation of approximately 600 (8hrs use/day)-1000 (4hrs use/day) hours, in addition to supporting reliable, multi-modal, subtle inputs. Our technical evaluation shows the strong robustness of the ring-to-wristband wireless link against different users, hand postures, and potential situations in the field of wearable computing. We strongly believe picoRing *mouse* could provide a new class of long-term wearables, seamlessly interconnecting itself with daily HCI devices.

Acknowledgments

This work was supported by JST ACT-X JPMJAX21K9, JSPS KAKEN 22K21343, JST ASPIRE JPMJAP2401, and Asahi Glass Foundation.

References

[1] Daniel Ashbrook, Patrick Baudisch, and Sean White. 2011. Nenya: subtle and eyes-free mobile input with a magnetically-tracked finger ring. In *Proceedings of the SIGCHI Conference on Human Factors in Computing Systems*. ACM, Vancouver BC Canada, 2043–2046. https://doi.org/10.1145/1978942.1979238

[2] Rachel Bainbridge and Joseph A. Paradiso. 2011. Wireless Hand Gesture Capture through Wearable Passive Tag Sensing. In *2011 International Conference on Body Sensor Networks*. 200–204. https://doi.org/10.1109/BSN.2011.42 ISSN: 2376-8894.

[3] Liwei Chan, Yi-Ling Chen, Chi-Hao Hsieh, Rong-Hao Liang, and Bing-Yu Chen. 2015. CyclopsRing: Enabling Whole-Hand and Context-Aware Interactions Through a Fisheye Ring. In *Proceedings of the 28th Annual ACM Symposium on User Interface Software & Technology*. ACM, Charlotte NC USA, 549–556. https://doi.org/10.1145/2807442.2807450

[4] Taizhou Chen, Tianpei Li, Xingyu Yang, and Kening Zhu. 2022. EFRing: Enabling Thumb-to-Index-Finger Microgesture Interaction through Electric Field Sensing Using Single Smart Ring. *Proceedings of the ACM on Interactive, Mobile, Wearable and Ubiquitous Technologies* 6, 4 (Dec. 2022), 1–31. https://doi.org/10.1145/3569478

[5] Michele Clarke. 1994. Spectrum Ring Mouse. https://www.microsoft.com/buxtoncollection/detail.aspx?id=19

[6] Bruce Cook and I. J Lowe. 1982. A large-inductance, high-frequency, high-*Q*, series-tuned coil for NMR. *Journal of Magnetic Resonance (1969)* 49, 2 (Sept. 1982), 346–349. https://doi.org/10.1016/0022-2364(82)90200-1

[7] Artem Dementyev and Joseph A. Paradiso. 2014. WristFlex: low-power gesture input with wrist-worn pressure sensors. In *Proceedings of the 27th annual ACM symposium on User interface software and technology*. ACM, Honolulu Hawaii USA, 161–166. https://doi.org/10.1145/2642918.2647396

[8] Joshua F. Ensworth and Matthew S. Reynolds. 2017. BLE-Backscatter: Ultralow-Power IoT Nodes Compatible With Bluetooth 4.0 Low Energy (BLE) Smartphones and Tablets. *IEEE Transactions on Microwave Theory and Techniques* 65, 9 (Sept. 2017), 3360–3368. https://doi.org/10.1109/TMTT.2017.2687866 Conference Name: IEEE Transactions on Microwave Theory and Techniques.

[9] Masaaki Fukumoto and Yasuhito Suenaga. 1994. "FingeRing": a full-time wearable interface. In *Conference companion on Human factors in computing systems - CHI '94*. ACM Press, Boston, Massachusetts, United States, 81–82. https://doi.org/10.1145/259963.260056

[10] Masaaki Fukumoto and Yoshinobu Tonomura. 1997. "Body coupled FingerRing": wireless wearable keyboard. In *Proceedings of the ACM SIGCHI Conference on Human factors in computing systems*. ACM, Atlanta Georgia USA, 147–154. https://doi.org/10.1145/258549.258636

[11] Fredric Gerr, Michele Marcus, Cindy Ensor, David Kleinbaum, Susan Cohen, Alicia Edwards, Eileen Gentry, Daniel J. Ortiz, and Carolyn Monteilh. 2002. A prospective study of computer users: I. Study design and incidence of musculoskeletal symptoms and disorders. *American Journal of Industrial Medicine* 41, 4 (April 2002), 221–235. https://doi.org/10.1002/ajim.10066

[12] Francisco Javier González-Cañete and Eduardo Casilari. 2021. A Feasibility Study of the Use of Smartwatches in Wearable Fall Detection Systems. *Sensors* 21, 6 (Jan. 2021), 2254. https://doi.org/10.3390/s21062254 Number: 6 Publisher: Multidisciplinary Digital Publishing Institute.

[13] Jeremy Gummeson, Bodhi Priyantha, and Jie Liu. 2014. An energy harvesting wearable ring platform for gestureinput on surfaces. In *Proceedings of the 12th annual international conference on Mobile systems, applications, and services*. ACM, Bretton Woods New Hampshire USA, 162–175. https://doi.org/10.1145/2594368.2594389

[14] Shuo Jiang, Peiqi Kang, Xinyu Song, Benny P.L. Lo, and Peter B. Shull. 2022. Emerging Wearable Interfaces and Algorithms for Hand Gesture Recognition: A Survey. *IEEE Reviews in Biomedical Engineering* 15 (2022), 85–102. https://doi.org/10.1109/RBME.2021.3078190 Conference Name: IEEE Reviews in Biomedical Engineering.

[15] Lei Jing, Yinghui Zhou, Zixue Cheng, and Tongjun Huang. 2012. Magic Ring: A Finger-Worn Device for Multiple Appliances Control Using Static Finger Gestures. *Sensors* 12, 5 (May 2012), 5775–5790. https://doi.org/10.3390/s120505775 Number: 5 Publisher: Molecular Diversity Preservation International.

[16] Ayato Kanada, Ryo Takahashi, Keito Hayashi, Ryusuke Hosaka, Wakako Yukita, Yasutaka Nakashima, Tomoyuki Yokota, Takao Someya, Mitsuhiro Kamezaki, Yoshihiro Kawahara, and Motoji Yamamoto. 2025. Joint-repositionable Inner-wireless Planar Snake Robot. *IEEE Robotics and Automation Letters* (2025), 1–8. https://doi.org/10.1109/LRA.2025.3555394 Conference Name: IEEE Robotics and Automation Letters.

[17] Mohamed Kari and Christian Holz. 2023. HandyCast: Phone-based Bimanual Input for Virtual Reality in Mobile and Space-Constrained Settings via Pose-and-Touch Transfer. In *Proceedings of the 2023 CHI Conference on Human Factors in Computing Systems*. ACM, Hamburg Germany, 1–15. https://doi.org/10.1145/3544548.3580677

[18] Rohde & Schwarz GmbH & Co KG. [n. d.]. Near Field Communication (NFC) Technology and Measurements. https://www.rohde-schwarz.com/us/applications/near-field-communication-nfc-technology-and-measurements-white-paper_230854-15836.html

[19] Wolf Kienzle and Ken Hinckley. 2014. LightRing: always-available 2D input on any surface. In *Proceedings of the 27th annual ACM symposium on User interface software and technology*. ACM, Honolulu Hawaii USA, 157–160. https://doi.org/10.1145/2642918.2647376

[20] Wolf Kienzle, Eric Whitmire, Chris Rittaler, and Hrvoje Benko. 2021. ElectroRing: Subtle Pinch and Touch Detection with a Ring. In *Proceedings of the 2021 CHI Conference on Human Factors in Computing Systems*. ACM, Yokohama Japan, 1–12. https://doi.org/10.1145/3411764.3445094

[21] Daehwa Kim and Chris Harrison. 2022. EtherPose: Continuous Hand Pose Tracking with Wrist-Worn Antenna Impedance Characteristic Sensing. In *Proceedings of the 35th Annual ACM Symposium on User Interface Software and Technology*. ACM, Bend OR USA, 1–12. https://doi.org/10.1145/3526113.3545665

[22] Maruchi Kim, Antonio Glenn, Bandhav Veluri, Yunseo Lee, Eyoel Gebre, Aditya Bagaria, Shwetak Patel, and Shyamnath Gollakota. 2024. IRIS: Wireless ring for vision-based smart home interaction. In *Proceedings of the 37th Annual ACM Symposium on User Interface Software and Technology*. ACM, Pittsburgh PA USA, 1–16. https://doi.org/10.1145/3654777.3676327

[23] Gierad Laput, Robert Xiao, and Chris Harrison. 2016. ViBand: High-Fidelity Bio-Acoustic Sensing Using Commodity Smartwatch Accelerometers. In *Proceedings of the 29th Annual Symposium on User Interface Software and Technology*. ACM, Tokyo Japan, 321–333. https://doi.org/10.1145/2984511.2984582

[24] Chi-Jung Lee, Rong-Hao Liang, Ling-Chien Yang, Chi-Huan Chiang, Te-Yen Wu, and Bing-Yu Chen. 2022. NFCStack: Identifiable Physical Building Blocks that Support Concurrent Construction and Frictionless Interaction. In *Proceedings of the 35th Annual ACM Symposium on User Interface Software and Technology*. ACM, Bend OR USA, 1–12. https://doi.org/10.1145/3526113.3545658

[25] Jiamin Li, Yilong Dong, Jeong Hoan Park, and Jerald Yoo. 2021. Body-coupled power transmission and energy harvesting. *Nature Electronics* 4, 7 (July 2021), 530–538. https://doi.org/10.1038/s41928-021-00592-y Publisher: Nature Publishing Group.

[26] Yifan Li, Masaaki Fukumoto, Mohamed Kari, Tomoyuki Yokota, Takao Someya, Yoshihiro Kawahara, and Ryo Takahashi. 2025. Demo of picoRing mouse: an ultra-low-powered wireless mouse ring with ring-to-wristband coil-based impedance sensing. https://doi.org/10.1145/3706599.3721183 arXiv:2501.16674 [cs].

[27] Yifan Li, Ryo Takahashi, Wakako Yukita, Kanata Matsutani, Cedric Caremel, Yuhiro Iwamoto, Sunghoon Lee, Tomoyuki Yokota, Takao Someya, and Yoshihiro Kawahara. 2025. Plug-n-play e-knit: prototyping large-area e-textiles using machine-knitted magnetically-repositionable sensor networks. In *Proceedings of the Nineteenth International Conference on Tangible, Embedded, and Embodied Interaction (TEI '25)*. Association for Computing Machinery, New York, NY, USA, 1–7. https://doi.org/10.1145/3689050.3705973

[28] Chen Liang, Chun Yu, Yue Qin, Yuntao Wang, and Yuanchun Shi. 2021. DualRing: Enabling Subtle and Expressive Hand Interaction with Dual IMU Rings. *Proceedings of the ACM on Interactive, Mobile, Wearable and Ubiquitous Technologies* 5, 3 (Sept. 2021), 1–27. https://doi.org/10.1145/3478114

[29] Rong-Hao Liang and Zengrong Guo. 2021. NFCSense: Data-Defined Rich-ID Motion Sensing for Fluent Tangible Interaction Using a Commodity NFC Reader. In *Proceedings of the 2021 CHI Conference on Human Factors in Computing Systems (CHI '21)*. Association for Computing Machinery, New York, NY, USA, 1–14.

https://doi.org/10.1145/3411764.3445214

[30] Vincent Liu, Aaron Parks, Vamsi Talla, Shyamnath Gollakota, David Wetherall, and Joshua R. Smith. 2013. Ambient backscatter: wireless communication out of thin air. In *Proceedings of the ACM SIGCOMM 2013 conference on SIGCOMM*. ACM, Hong Kong China, 39–50. https://doi.org/10.1145/2486001.2486015

[31] Sigurd Mikkelsen, Imogen Vilstrup, Christina Funch Lassen, Ann Isabel Kryger, Jane Frølund Thomsen, and Johan Hviid Andersen. 2007. Validity of questionnaire self-reports on computer, mouse and keyboard usage during a four-week period. *Occupational and Environmental Medicine* 64, 8 (Aug. 2007), 541–547. https://doi.org/10.1136/oem.2005.026351

[32] Saman Naderiparizi, Mehrdad Hessar, Vamsi Talla, Shyamnath Gollakota, and Joshua R. Smith. 2018. Towards {Battery-Free} {HD} Video Streaming. 233–247. https://www.usenix.org/conference/nsdi18/presentation/naderiparizi

[33] Farshid Salemi Parizi, Eric Whitmire, and Shwetak Patel. 2019. AuraRing: Precise Electromagnetic Finger Tracking. *Proceedings of the ACM on Interactive, Mobile, Wearable and Ubiquitous Technologies* 3, 4 (Dec. 2019), 1–28. https://doi.org/10.1145/3369831

[34] J. Rekimoto. 2001. GestureWrist and GesturePad: unobtrusive wearable interaction devices. In *Proceedings Fifth International Symposium on Wearable Computers*. IEEE Comput. Soc, Zurich, Switzerland, 21–27. https://doi.org/10.1109/ISWC.2001.962092

[35] T. Scott Saponas, Desney S. Tan, Dan Morris, Ravin Balakrishnan, Jim Turner, and James A. Landay. 2009. Enabling always-available input with muscle-computer interfaces. In *Proceedings of the 22nd annual ACM symposium on User interface software and technology*. ACM, Victoria BC Canada, 167–176. https://doi.org/10.1145/1622176.1622208

[36] Takashi Sato, Shinto Watanabe, Ryo Takahashi, Wakako Yukita, Tomoyuki Yokota, Takao Someya, Yoshihito Kawahara, Eiji Iwase, and Junya Kurumida. 2025. Friction Jointing Of Distributed Rigid Capacitors To Stretchable Liquid Metal Coil For Full-Body Wireless Charging Clothing. In *2025 IEEE 38th International Conference on Micro Electro Mechanical Systems (MEMS)*. 181–184. https://doi.org/10.1109/MEMS61431.2025.10917417 ISSN: 2160-1968.

[37] Xiyuan Shen, Chun Yu, Xutong Wang, Chen Liang, Haozhan Chen, and Yuanchun Shi. 2024. MouseRing: Always-available Touchpad Interaction with IMU Rings. In *Proceedings of the CHI Conference on Human Factors in Computing Systems*. ACM, Honolulu HI USA, 1–19. https://doi.org/10.1145/3613904.3642225

[38] Wei Sun, Franklin Mingzhe Li, Congshu Huang, Zhenyu Lei, Benjamin Steeper, Songyun Tao, Feng Tian, and Cheng Zhang. 2021. ThumbTrak: Recognizing Micro-finger Poses Using a Ring with Proximity Sensing. In *Proceedings of the 23rd International Conference on Mobile Human-Computer Interaction*. ACM, Toulouse & Virtual France, 1–9. https://doi.org/10.1145/3447526.3472060

[39] Ryo Takahashi, Masaaki Fukumoto, Changyo Han, Takuya Sasatani, Yoshiaki Narusue, and Yoshihiro Kawahara. 2020. TelemetRing: A Batteryless and Wireless Ring-shaped Keyboard using Passive Inductive Telemetry. In *Proceedings of the 33rd Annual ACM Symposium on User Interface Software and Technology*. ACM, Virtual Event USA, 1161–1168. https://doi.org/10.1145/3379337.3415873

[40] Ryo Takahashi, Changyo Han, Wakako Yukita, John S. Ho, Takuya Sasatani, Akihito Noda, Tomoyuki Yokota, Takao Someya, and Yoshihiro Kawahara. 2025. Full-body NFC: body-scale near-field sensor networks with machine-knittable meandered e-textiles. https://doi.org/10.48550/arXiv.2503.13240 arXiv:2503.13240 [cs].

[41] Ryo Takahashi, Eric Whitmire, Roger Boldu, Shiu Ng, Wolf Kienzle, and Hrvoje Benko. 2024. picoRing: battery-free rings for subtle thumb-to-index input. In *Proceedings of the 37th Annual ACM Symposium on User Interface Software and Technology*. ACM, Pittsburgh PA USA, 1–11. https://doi.org/10.1145/3654777.3676365

[42] Ryo Takahashi, Wakako Yukita, Takuya Sasatani, Tomoyuki Yokota, Takao Someya, and Yoshihiro Kawahara. 2021. Twin Meander Coil: Sensitive Readout of Battery-free On-body Wireless Sensors Using Body-scale Meander Coils. *Proceedings of the ACM on Interactive, Mobile, Wearable and Ubiquitous Technologies* 5, 4 (Dec. 2021), 1–21. https://doi.org/10.1145/3494996

[43] Ryo Takahashi, Wakako Yukita, Tomoyuki Yokota, Takao Someya, and Yoshihiro Kawahara. 2022. Meander Coil++: A Body-scale Wireless Power Transmission Using Safe-to-body and Energy-efficient Transmitter Coil. In *CHI Conference on Human Factors in Computing Systems*. ACM, New Orleans LA USA, 1–12. https://doi.org/10.1145/3491102.3502119

[44] Virag Varga, Marc Wyss, Gergely Vakulya, Alanson Sample, and Thomas R. Gross. 2018. Designing Groundless Body Channel Communication Systems: Performance and Implications. In *Proceedings of the 31st Annual ACM Symposium on User Interface Software and Technology (UIST '18)*. Association for Computing Machinery, New York, NY, USA, 683–695. https://doi.org/10.1145/3242587.3242622

[45] Nicolas Villar, Shahram Izadi, Dan Rosenfeld, Hrvoje Benko, John Helmes, Jonathan Westhues, Steve Hodges, Eyal Ofek, Alex Butler, Xiang Cao, and Billy Chen. 2009. Mouse 2.0: multi-touch meets the mouse. In *Proceedings of the 22nd annual ACM symposium on User interface software and technology (UIST '09)*. Association for Computing Machinery, New York, NY, USA, 33–42. https://doi.org/10.1145/1622176.1622184

[46] Anandghan Waghmare, Youssef Ben Taleb, Ishan Chatterjee, Arjun Narendra, and Shwetak Patel. 2023. Z-Ring: Single-Point Bio-Impedance Sensing for Gesture, Touch, Object and User Recognition. In *Proceedings of the 2023 CHI Conference on Human Factors in Computing Systems*. ACM, Hamburg Germany, 1–18. https://doi.org/10.1145/3544548.3581422

[47] Mahmoud Wagih, Leonardo Balocchi, Francesca Benassi, Nuno B. Carvalho, Jung-Chih Chiao, Ricardo Correia, Alessandra Costanzo, Yepu Cui, Dimitra Georgiadou, Carolina Gouveia, Jasmin Grosinger, John S. Ho, Kexin Hu, Abiodun Komolafe, Sam Lemey, Caroline Loss, Gaetano Marrocco, Paul Mitcheson, Valentina Palazzi, Nicoletta Panunzio, Giacomo Paolini, Pedro Pinho, Josef Preishuber-Pflügl, Yasser Qaragoez, Hamed Rahmani, Hendrik Rogier, Jose Romero Lopera, Luca Roselli, Dominique Schreurs, Manos Tentzeris, Xi Tian, Russel Torah, Ricardo Torres, Patrick Van Torre, Dieff Vital, and Steve Beeby. 2023. Microwave-Enabled Wearables: Underpinning Technologies, Integration Platforms, and Next-Generation Roadmap. *IEEE Journal of Microwaves* 3, 1 (Jan. 2023), 193–226. https://doi.org/10.1109/JMW.2022.3223254 Conference Name: IEEE Journal of Microwaves.

[48] Mingke Wang, Qing Luo, Yasha Iravantchi, Xiaomeng Chen, Alanson Sample, Kang G. Shin, Xiaohua Tian, Xinbing Wang, and Dongyao Chen. 2022. Automatic calibration of magnetic tracking. In *Proceedings of the 28th Annual International Conference on Mobile Computing And Networking (MobiCom '22)*. Association for Computing Machinery, New York, NY, USA, 391–404. https://doi.org/10.1145/3495243.3558760

[49] Brian S. Wolff, Sumiyya A. Raheem, and Leorey N. Saligan. 2018. Comparing passive measures of fatigue-like behavior in mice. *Scientific Reports* 8 (Sept. 2018), 14238. https://doi.org/10.1038/s41598-018-32654-1

[50] Chenhan Xu, Bing Zhou, Gurunandan Krishnan, and Shree Nayar. 2023. AO-Finger: Hands-free Fine-grained Finger Gesture Recognition via Acoustic-Optic Sensor Fusing. In *Proceedings of the 2023 CHI Conference on Human Factors in Computing Systems*. ACM, Hamburg Germany, 1–14. https://doi.org/10.1145/3544548.3581264

[51] Tianhong Catherine Yu, Guilin Hu, Ruidong Zhang, Hyunchul Lim, Saif Mahmud, Chi-Jung Lee, Ke Li, Devansh Agarwal, Shuyang Nie, Jinseok Oh, François Guimbretière, and Cheng Zhang. 2024. Ring-a-Pose: A Ring for Continuous Hand Pose Tracking. *Proceedings of the ACM on Interactive, Mobile, Wearable and Ubiquitous Technologies* 8, 4 (Nov. 2024), 1–30. https://doi.org/10.1145/3699741

[52] Jun-Lin Zhan, Wei-Bing Lu, Cong Ding, Zhen Sun, Bu-Yun Yu, Lu Ju, Xin-Hua Liang, Zhao-Min Chen, Hao Chen, Yong-Hao Jia, Zhen-Guo Liu, and Tie-Jun Cui. 2024. Flexible and wearable battery-free backscatter wireless communication system for colour imaging. *npj Flexible Electronics* 8, 1 (March 2024), 1–9. https://doi.org/10.1038/s41528-024-00304-4 Publisher: Nature Publishing Group.

[53] Cheng Zhang, Anandghan Waghmare, Pranav Kundra, Yiming Pu, Scott Gilliland, Thomas Ploetz, Thad E. Starner, Omer T. Inan, and Gregory D. Abowd. 2017. FingerSound: Recognizing unistroke thumb gestures using a ring. *Proceedings of the ACM on Interactive, Mobile, Wearable and Ubiquitous Technologies* 1, 3 (Sept. 2017), 1–19. https://doi.org/10.1145/3130985

[54] Junbo Zhang, Gaurav Balakrishnan, Sruti Srinidhi, Arnav Bhat, Swarun Kumar, and Christopher Bettinger. 2022. NFCapsule: An Ingestible Sensor Pill for Eosinophilic Esophagitis Detection Based on near-Field Coupling. In *Proceedings of the 20th ACM Conference on Embedded Networked Sensor Systems*. ACM, Boston Massachusetts, 75–90. https://doi.org/10.1145/3560905.3568523

[55] Yang Zhang, Robert Xiao, and Chris Harrison. 2016. Advancing Hand Gesture Recognition with High Resolution Electrical Impedance Tomography. In *Proceedings of the 29th Annual Symposium on User Interface Software and Technology*. ACM, Tokyo Japan, 843–850. https://doi.org/10.1145/2984511.2984574

[56] Yuliang Zhao, Jiali Liu, Chao Lian, Yifan Liu, Xianshou Ren, Jiazhi Lou, Meng Chen, and Wen Jung Li. 2022. A Single Smart Ring for Monitoring 20 Kinds of Multi-Intensity Daily Activities––From Kitchen Work to Fierce Exercises. *Advanced Intelligent Systems* 4, 12 (2022), 2200204. https://doi.org/10.1002/aisy.202200204 _eprint: https://onlinelibrary.wiley.com/doi/pdf/10.1002/aisy.202200204.

[57] Yi Zhao, Joshua R. Smith, and Alanson Sample. 2015. NFC-WISP: A sensing and computationally enhanced near-field RFID platform. In *2015 IEEE International Conference on RFID (RFID)*. 174–181. https://doi.org/10.1109/RFID.2015.7113089 ISSN: 2374-0221.

[58] Hao Zhou, Taiting Lu, Yilin Liu, Shijia Zhang, Runze Liu, and Mahanth Gowda. 2023. One Ring to Rule Them All: An Open Source Smartring Platform for Finger Motion Analytics and Healthcare Applications. In *Proceedings of the 8th ACM/IEEE Conference on Internet of Things Design and Implementation*. ACM, San Antonio TX USA, 27–38. https://doi.org/10.1145/3576842.3582382

Received 20 February 2007; revised 12 March 2009; accepted 5 June 2009